Frontiers of Information Technology & Electronic Engineering
www.jzus.zju.edu.cn; engineering.cae.cn; www.springerlink.com
ISSN 2095-9184 (print); ISSN 2095-9230 (online)
E-mail: jzus@zju.edu.cn

Review:

Light field imaging: models, calibrations, reconstructions, and applications*

Hao ZHU[1], Qing WANG[†‡1], Jingyi YU[2]

([1]*School of Computer Science, Northwestern Polytechnical University, Xi'an 710072, China*)

([2]*School of Information Science and Technology, ShanghaiTech University, Shanghai 201210, China*)

[†]E-mail: qwang@nwpu.edu.cn

Received Nov. 20, 2016; Revision accepted Mar. 7, 2017; Crosschecked Sept. 6, 2017

Abstract: Light field imaging is an emerging technology in computational photography areas. Based on innovative designs of the imaging model and the optical path, light field cameras not only record the spatial intensity of three-dimensional (3D) objects, but also capture the angular information of the physical world, which provides new ways to address various problems in computer vision, such as 3D reconstruction, saliency detection, and object recognition. In this paper, three key aspects of light field cameras, i.e., model, calibration, and reconstruction, are reviewed extensively. Furthermore, light field based applications on informatics, physics, medicine, and biology are exhibited. Finally, open issues in light field imaging and long-term application prospects in other natural sciences are discussed.

Key words: Light field imaging; Plenoptic function; Imaging model; Calibration; Reconstruction
https://doi.org/10.1631/FITEE.1601727 **CLC number:** TP391.4

1 Introduction

Light is an electromagnetic wave distributed in space, which contains multiple types of information (such as amplitude, phase, and wavelength) and helps us perceive the position, color, light, and shade of an object in the three-dimensional (3D) world. However, this information is lost in the traditional integral imaging system because only the light intensity on a two-dimensional (2D) slice is recorded. Furthermore, the angular information that is related with scene structures, object shapes, and occlusions is mixed in a 2D position (spatial) image, which makes it difficult to recover the high-dimensional world from the low-dimensional 2D image in computer vision.

Inheriting the theories and designs from traditional systems, light field imaging records the spatial and angular information at the same time by innovating imaging models and improving hardware designs, as well as achieving novel imaging effects, such as digital refocusing, extended depth of fields (DOF), and multiperspective views. Light field imaging not only provides new ideas for obtaining high-quality visual information, but also helps us solve classic problems in computer vision better. Light field imaging has become a promising method to make breakthrough over the physical limits in the traditional integral imaging system.

The development trends in light field theory, technologies, and equipment are summarized in Fig. 1. Light field imaging can effectively improve the performance of digital imaging, such as DOF, view synthesis, and high dynamic range, and increase the accuracy and robustness of 3D recon-

‡ Corresponding author

* Project supported by the National Natural Science Foundation of China (Nos. 61531014 and 61272287)

ORCID: Hao ZHU, http://orcid.org/0000-0002-6756-9571; Qing WANG, http://orcid.org/0000-0003-3439-0644

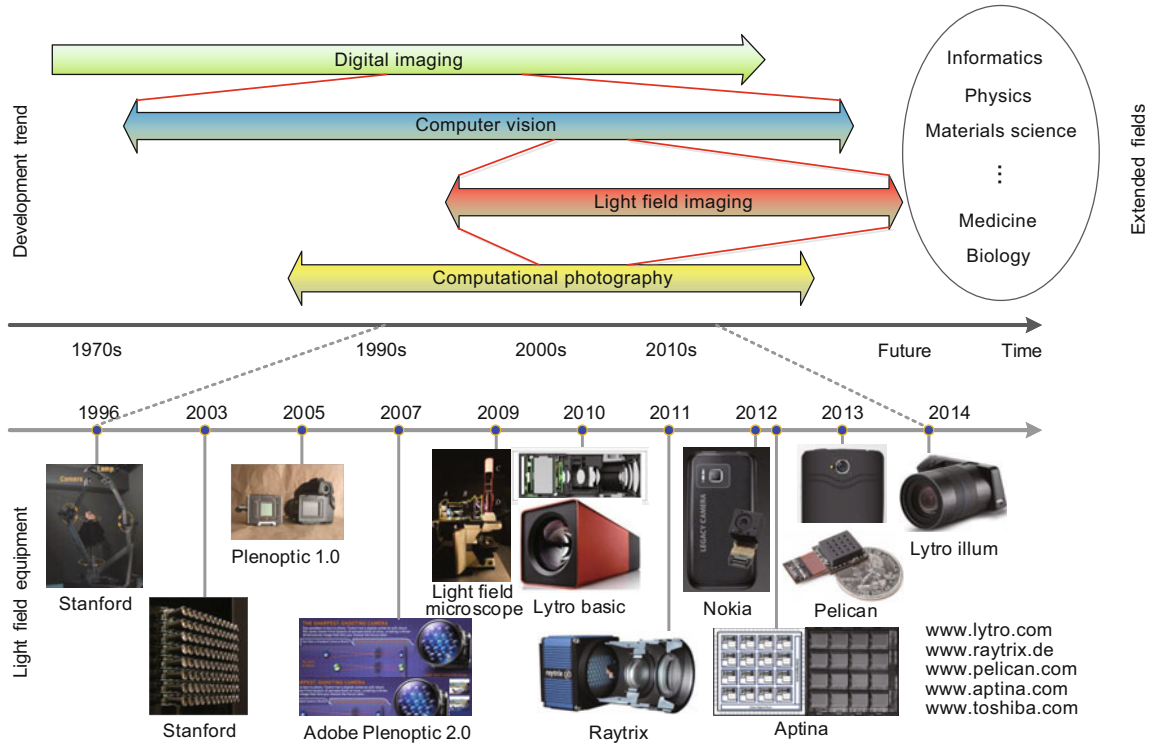

Fig. 1 Development trends of light field imaging theory, technologies, and equipment

struction, panorama stitching, object recognition, and object tracking in computer vision. Apart from computer science, the key technologies in light field imaging can be well extended to particle image velocimetry (PIV), analysis of structure of metallic/nonmetallic materials, and microscopic imaging, which promote the developments in informatics, physics, materials, medicine, and biology.

In this paper, we focus on three key aspects of light field imaging, including (1) light field imaging models and optical path designs, (2) calibration and optimization for light field cameras, and (3) reconstruction of the physical world using light field cameras. Then some newest applications from different disciplines based on light field imaging are introduced. Finally, we summarize the existing works in light field imaging and thereafter discuss open issues and possible research directions in the future.

2 Light field imaging models

To analyze the vision signal, namely, light rays, in geometric optics, Landy and Movshon (1991) modeled the continuous light field using a plenoptic function in the seven-dimensional (7D) space, i.e., $L(x, y, z, \theta, \phi, \lambda, t)$. For each ray in space at time t, (x, y, z) and (θ, ϕ) represent its geometric information, i.e., the position and direction respectively, and λ describes the wavelength. However, it is difficult to obtain a full 7D function in the real world such that the dimension is often decreased in different situations. When the scene is static, we can remove t from the equation. By assuming that the intensity is not attenuated (Gortler *et al.*, 1996; Levoy and Hanrahan, 1996), the 7D function is further decreased to a four-dimensional (4D) function, which can be described using plane–sphere, two-plane, and in-camera parameterization (Liang *et al.*, 2011).

With the progress in light field imaging theory, many devices have been developed to acquire the light field, such as the camera array (Wilburn, 2004), coded-aperture camera (Levin *et al.*, 2007), focal sweep camera (Zhou *et al.*, 2012), and microlens array (MLA) based camera (Ng *et al.*, 2005; Georgiev and Lumsdaine, 2010). Among all the devices, the MLA-based camera is the most promising, because it is inexpensive (the traditional camera can be easily converted to a light field camera by inserting an MLA between the main lens and the image sensor) and convenient (it is small and can provide

light field in a single shot). There are many kinds of MLA-based cameras or prototypes released by Lytro (www.lytro.com), Raytrix (www.raytrix.de), Pelican (Venkataraman *et al.*, 2013), Adobe (Georgiev and Lumsdaine, 2010), etc. In this section, we first review the light field representation and then compare two imaging models in the MLA-based cameras.

2.1 Light field representation

Unlike traditional 2D images, a light field image has a higher dimension and needs a more complex parameterized method. Levoy and Hanrahan (1996) pointed out that the 2D image captured by the traditional camera is just the projection of continuous light signals in the 2D subspace. Therefore, the famous two-parallel-plane (TPP) model has been proposed to represent the light field (Fig. 2), i.e., $L(x, y, u, v)$, where (x, y) and (u, v) denote the intersections of the light ray in the spatial and angular planes, respectively. Gortler *et al.* (1996) analyzed the lumigraph in a free space (no occlusion). By ignoring the attenuation in the propagation of rays, they have proven the equivalence between 4D light field parameterization and 5D light field signals. Liang *et al.* (2011) modeled the propagation of light rays, and pointed out that the plane–sphere, TPP, and in-camera parameterizations can equivalently represent the 4D light field. Yu and McMillan (2004) analyzed the imaging models of eight kinds of traditional cameras (perspective camera, orthographic camera, pushbroom camera, etc.) using the TPP model and showed that different camera models come from different strategies for dimensionality reduction and sampling.

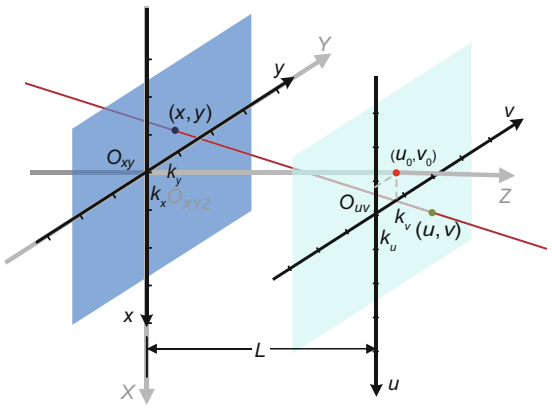

Fig. 2 Two-parallel-plane model and its parameters

Due to the conciseness of the TPP model, it is widely applied to the sampling of 4D light field, such as the camera array and MLA-based cameras. Isaksen *et al.* (2000) proposed a dynamic reparameterization algorithm to refocus the light field at different depths. Ng (2005) pointed out that refocusing in the spatial domain equals the 2D slice in the Fourier domain, which accelerates the obtaining of the focal stack. Vaish *et al.* (2005) further developed a method to refocus the light field in an inclined plane. Because the field-of-view (FOV) of monocular light field cameras is small, Birklbauer and Bimber (2014) proposed to stitch a panoramic light field by reparameterizing multiview light fields into a two-cylinder model.

As shown in Fig. 2, there are seven parameters in the TPP model, including the interval L between the two parallel planes, the offset (u_0, v_0) between the origins of the two 2D plane coordinates, and the four scaling factors (k_x, k_y, k_u, k_v) along the four axes. Thus, $\boldsymbol{H} = (L, k_x, k_y, k_u, k_v, u_0, v_0)^{\mathrm{T}}$ is the parameter vector of the TPP coordinates. The scale of the u–v plane (k_u, k_v) handles the projective transformation, and the scale of the x–y plane (k_x, k_y) handles the zoom of the recovered scene. The perspective relationship and distortions between a 3D cube and the 4D light field are shown in Fig. 3, where panel (a) shows an original cube and panels (b)–(d) show the distorted cubes obtained by changing L, $k_{uv}(= k_u = k_v)$, and (u_0, v_0), respectively.

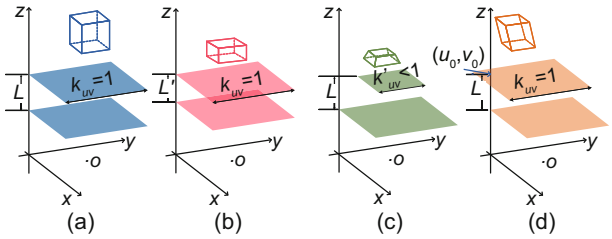

Fig. 3 Two-parallel-plane light field recording a Lambertian cube. Panel (a) is the original cube and panels (b)–(d) are the distorted cubes obtained with the change of L, $k_{uv}(= k_u = k_v)$, and (u_0, v_0), respectively

In brief, a light field can be well represented by a TPP model, which results in the accuracy of light field camera calibration. Seven parameters of the TPP model can totally constrain the perspective relationship and scaling between the light field and the 3D structure, and have important influences on 3D reconstructions from the light field.

2.2 Optical path design

The most important aspect of a plenoptic camera is the optical path design. Ng *et al.* (2005) proposed the first portable light field camera (Plenoptic 1.0). By inserting an MLA at the focal length of the main lens and placing the image sensor at the focal length of the microlens, light rays emitted from a point are recorded in the image sensor (Fig. 4a). The subimage covered by each microlens represents the angular sampling of a point. To make full use of pixels in the image sensor, it is essential to choose proper focal lengths for the microlens and main lens so as to ensure that no overlapping occurs and to minimize the gap between subimages.

As we know, the spatial resolution of Plenoptic 1.0 equals the number of the microlens, while the angular resolution equals the number of pixels covered by each microlens. To improve the spatial resolution, Lumsdaine and Georgiev (2008) designed a focused plenoptic camera (Plenoptic 2.0), in which the MLA can be placed at any position except the focal length of the main lens. The position of the image sensor is determined by the MLA configuration. Unlike angular sampling in Plenoptic 1.0, the microlens here records the in-camera 3D scene, which is conveyed from the main lens (secondary focusing) (Fig. 4b) or focusing in advance (Fig. 4c). All of these depend on the interval between the MLA and the main lens. In this model, the distances z and g between the main lens, the MLA, and the image sensor ought to meet the Gaussian imaging rule. Thus, the number of angular samplings M is determined by the expression $M = z/(kg)$, where k is determined by the arrangement of the MLA. The focused plenoptic camera can be regarded as a microcamera array, where each subimage covered by the microlens equals a local observation of the in-camera scene. Apart from this, Georgiev and Lumsdaine (2012) proposed a multifocus plenoptic camera, which was implemented by Perwaß and Perwaß (2013), i.e., Raytrix. The advantage of the multifocus plenoptic camera is a larger DOF, but the image quality and refocusing ability are degraded.

As shown in Fig. 4, the spatial and angular resolutions, i.e., sampling numbers, are determined by the position of each component, which can be changed by adjusting the relative positions of the components. However, regardless of how these components are adjusted, a trade-off between the spatial and angular resolutions still exists (Georgiev *et al.*, 2006). The breakthrough of the image sensor, e.g., a multilayer design, may thoroughly solve the bottleneck between the spatial and angular resolutions.

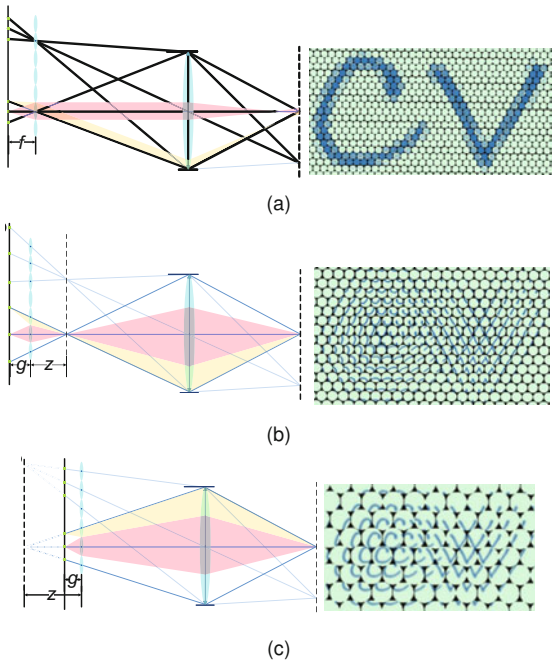

Fig. 4 Optical path and imaging effect: (a) Plenoptic 1.0; (b) Plenoptic 2.0 (secondary imaging); (c) Plenoptic 2.0 (focusing in advance)

In short, it is easy to decode light fields from a Plenoptic 1.0 camera with a higher angular but lower spatial resolution. The Plenoptic 2.0 camera provides a more flexible approach to balance the spatial and angular resolutions in 4D light field; nevertheless, it needs a more complex ray-decoding process.

3 Light field camera calibrations

Because light field cameras capture a 4D light field and rearrange it in a 2D image, it is more difficult to calibrate light field cameras than traditional ones. The objective of calibration of the traditional camera is to find the projective matrix $\boldsymbol{P}$ that relates a 2D image point $\boldsymbol{x}$ with the 3D point $\boldsymbol{X}$, i.e., $\boldsymbol{x} = \boldsymbol{P}\boldsymbol{X}$. Because the depth is implicitly embedded in the 2D image point in light field imaging by assigning different disparities to different points, it is essential to estimate the intrinsic and extrinsic parameters exactly. It is also important to rectify the

distortion in angular sampling.

3.1 Decoding of rays and rectification

Existing calibration methods regard the microlens and main lens as a pinhole and thin lens model, respectively. The 4D TPP light field, which is acquired by a light field camera, equals the multiview images captured by a camera array (all optical centers of elemental lenses are on the same plane). Therefore, light field decoding can be modeled as the combination of multiview images and it leads to different decoding methods for light rays.

There are two ways to describe a unique ray in the 3D space, including the 4D TPP representation and the 6D Plücker parameterized method. For Plenoptic 1.0, Dansereau *et al.* (2013) proposed an intrinsic parameter matrix to project the subimage $(i,j,k,l)^{\mathrm{T}}$ to the ray vector $(s,t,u,v)^{\mathrm{T}}$ in the TPP coordinates. For Plenoptic 2.0, Perwaß and Wietzke (2012) defined each image pixel as the ray that passes through the image sensor plane and the optical center of the microlens and then refocused the light field using ray tracing, which has the same physical meaning as that proposed by Georgiev and Lumsdaine (2010) and Wanner *et al.* (2011). Bergamasco *et al.* (2015) decoded the 4D light field using a coded color pattern, which reflects different colors in different angles, and improved the reconstruction accuracy of the coded color pattern.

In ray decoding, Ng (2006) proposed a typical algorithm to decode the 4D light field from a Plenoptic 1.0 camera, which equals the decoding of a TPP light field without the constraint L. Hahne *et al.* (2014) skipped the 4D light field decoding and generated the refocused image by rearranging raw data. It is noticed that some rays are directly decoded from the raw data, considering the discrete sampling pattern of color in the image sensor. Sabater *et al.* (2014) directly generated multiview images from raw data without demosaicing. Yu *et al.* (2012) proposed a Fourier domain based method to first decode raw data and then to demosaic multiview images. Seifi *et al.* (2014) decoded multiview images that lack values in some channels first, and then generated the disparity map, which was used as a reference to improve image quality. Considering the limited band of light field sampling in a Plenoptic 2.0 camera, Georgiev and Lumsdaine (2009) and Georgiev *et al.* (2011) refocused the light field by changing the selected size of each subimage and generated multiview images by changing the weights for the rays in different angles.

However, all the aforementioned methods ignore the calibration of L and the ratio of the scaling factor k_x/k_u in the TPP model, which results in the shrinks shown in Figs. 3b and 3c. These distortions directly affect the accuracy of an absolute depth map. In addition, all these methods idealize the offsets of the principal points of the microlens, which leads to a larger aberration far away from the center. Hahne *et al.* (2015) verified the influence of the ray direction led by the shift in the principal point of the microlens by comparing the refocusing distance with the real depth.

The distortion model of a light field camera is more complex because more angular samplings are recorded. Dansereau *et al.* (2013) and Bok *et al.* (2014) considered the radial distortion, which holds that the offsets of light rays in the angular plane are related to its distance to the original position. Johannsen *et al.* (2013) explained the refraction using the Petzval surface and proposed an algorithm to eliminate depth distortion. Jeon *et al.* (2015) calculated the offset between multiview images and rectified the distortion according to the errors between the disparity map and scene priors. Zhang *et al.* (2016) proposed a four-parameter model to simplify the light field geometry and rectify plenoptic projective distortion.

3.2 Parameter solving methods

Each light ray in the 3D space is represented using two 2D coordinates in the classic TPP model. Previous works (Ng, 2005; Liang *et al.*, 2011; Dansereau *et al.*, 2013; Hahne *et al.*, 2014) have derived the spatial and Fourier representations of the TPP light field in different situations, including translation, rotation, projection, refraction, and occlusion.

Before parameter solving, it is essential to preprocess the raw light field data, such as subimage extraction, light field sampling, and generation of multiview images. Cho *et al.* (2013) rectified the raw light field data by locating the center of the microlens using a white scene. Jeon *et al.* (2015) aligned multiview images according to the errors between the disparity map and the priors of scene structure. Because these methods generate multiview images in

two directions, i.e., $L(x, y, u_i, v_i)$, but ignore L and the ratio of the scaling factor k_x/k_u, they cannot rearrange multiview images into a TPP light field with a unique parameter. Although the effects of light field rendering are not influenced, e.g., refocusing and view stitching, the absolute angles of the light ray cannot be represented due to the lack of these constraints.

Dansereau *et al.* (2013) used the pinhole and thin lens model to describe the microlens and main lens in Plenoptic 1.0 and proposed the projection matrix with 15 parameters to map the raw data to a 4D light field. The key factor, reprojection error, is defined as the distance between the real point and reconstructed ray. However, the initial solution is dependent on traditional camera calibration, and it considers only radial distortion. In particular, the model rectifies only the rotation on the image plane but ignores the pitch and tilt angles between the MLA and the main lens, which leads to inaccurate decoding. Bok *et al.* (2014) calibrated light field cameras by extracting feature lines from raw data directly. The initial value is obtained using these feature lines, and the intrinsic matrix and distortion are obtained via nonlinear optimization.

Thomason *et al.* (2014) further considered the offset between the centers of the subimage and the corresponding microlens, and thereby derived the association matrix between the MLA pose and the subimages' centers. The interval L and the 3D directional angle errors were calibrated by capturing a scene-aware star image. However, the accuracy was heavily influenced by the DOF, and it was difficult to guarantee the pose of the scene. Afterward, Johannsen *et al.* (2013) proposed a similar model with 21 parameters to calibrate the focused plenoptic camera. The depth distortion of the main lens was rectified using a Petzval surface, and the parameters were obtained using a nonlinear optimization algorithm. However, the offset of the principal point was neglected, which leads to errors when reconstructing the surface. Johannsen *et al.* (2015) further analyzed the related model of light rays in different TPP coordinates and registered multiview light fields to verify the accuracy of the model.

In summary, subimage extraction is the premise of light field camera calibration, and it is solved by capturing white images in almost all of the existing methods. So far, most of the works have focused on intrinsic parameter calibration, and there are only a few works on extrinsic parameters.

4 Light field reconstruction

The most significant feature of light field cameras is multiview imaging in a single shot, which increases angular sampling by decreasing spatial resolution. Herein, two important issues, depth estimation and super-resolution (SR) reconstruction, have arisen in the light field. In this section, we review the most representative approaches on the two problems.

4.1 Depth estimation

Depth estimation is a fundamental problem in computer vision, and many approaches from different depth cues have been proposed in different imaging conditions, such as stereo matching, photometric stereo, and depth from focus/defocus (DFF/DFD). Different methods are applied in different areas, but it is difficult to combine all methods into a unified framework for traditional imaging systems. Fortunately, all these depth cues are embedded in the light field imaging. With the microlens array, the light field imaging system splits light beams into different rays. The convergence of the rays at different refocused depths forms the focal stack, which is suitable for DFF/DFD (Lin *et al.*, 2015). The image formed from rays of the same angle constructs a multiview representation, which is suitable for stereo matching (Kim *et al.*, 2013; Yu *et al.*, 2013; Chen *et al.*, 2014; Jeon *et al.*, 2015; Williem and Park, 2016). Because the construction of the disparity image space in multiview stereo matching is also implemented by the refocus operation, the two methods are unified as refocusing-based methods (Tao *et al.*, 2013; Wang *et al.*, 2015). Additionally, rich angular resolution in the light field forms an epipolar plane image (EPI). Because the slope of the EPI line has a linear relationship with the depth, orientation analysis in EPI becomes a new trend to estimate the depth in the light field (Wanner and Goldluecke, 2012a; 2014; Tosic and Berkner, 2014; Li *et al.*, 2015; Johannsen *et al.*, 2016; Maximilian, 2016). For the areas that meet the Lambertian assumption and have sufficient textures, all methods can produce reliable depth maps. The current concern is how to handle the occlusion, noise, and glossy surface.

4.1.1 Occlusion

Occlusion is a common phenomenon and widely exists in natural scenes, especially in object boundaries, as shown in Fig. 5. The photo-consistency assumption fails in occlusion areas because these points cannot be observed from all views. Blindly applying photo-consistency may lead to oversmooth results in object boundaries.

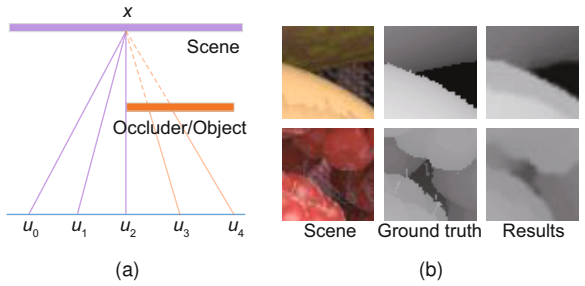

Fig. 5 Occlusion condition and the oversmooth results: (a) occlusion between views; (b) oversmooth results

There are many approaches for occlusion handling in the literature. With an initial 4D depth estimation using a structure tensor, Wanner and Goldluecke (2014) optimized the occlusion using global labeling constraints. However, because the tensor field becomes too random to be analyzed in occlusion boundaries, the global labeling constraints cannot provide satisfactory results. Yu *et al.* (2013) derived the constrained Delaunay triangulation of 3D lines in the 4D light field space. On this basis, they introduced the line-assisted graph cuts to improve depth estimation. However, the 3D lines were partitioned into small and incoherent segments, resulting in wrong estimation. These two methods notice only the appearance of occlusion but do not realize the cause of occlusion formation. Thus, the results are still oversmoothed in the occlusion boundaries.

Chen *et al.* (2014) first realized that although the photo-consistency assumption does not hold for all views, it holds for a part of views, i.e., the unoccluded views. On this basis, a bilateral consistency metric (BCM) has been proposed to measure the possibility of unoccluded views so that the most likely unoccluded views are selected for depth estimation. This work involves the occlusion but lacks the occlusion model. Wang *et al.* (2015) analyzed the formation of occlusion in the light field. By making the prior assumption of single-occluder occlusion, they found that the projection consistency between the spatial and the angular patches in occlusion boundaries, i.e., the line separating the occluded/unoccluded views in the angular space, has the same orientation as the edge in the spatial space (Fig. 6). Using this consistency, the unoccluded views are selected according to the edge orientation, and then these unoccluded views are encoded into the data and the smooth terms of the global minimization energy function.

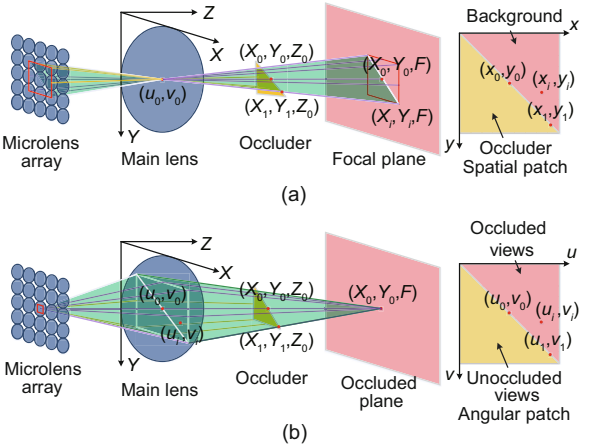

Fig. 6 Projection consistency between the spatial and angular patches in occlusion boundaries: (a) pinhole model; (b) 'reversed' pinhold model

The root mean square (RMS) errors of disparity estimation of the state-of-the-art techniques on the public synthetic light field data sets (Wanner *et al.*, 2013) are listed in Table 1, from which we find that Chen *et al.* (2014) achieved the best result. For real light field data captured by the Lytro or Lytro illum, due to the lack of ground truth depth, Wang *et al.* (2015) obtained the best result in qualitative comparison.

4.1.2 Noise

Due to the ultrasmall aperture of the microlens in light field cameras (14 μm in Lytro, 20 μm in Lytro illum, and 50 μm in Raytrix), the captured light field image has a low signal-to-noise ratio (SNR), which makes the state-of-the-art algorithms fail on real data. A common solution to reduce the influence of noise is to select as many views as possible. However, there are trade-offs in this solution; i.e., too many views lead to oversmooth occlusion boundaries and fewer views decrease the robustness in noisy areas.

Table 1 Root mean square (RMS) errors of disparity estimation of state-of-the-art techniques

Reference	RMS error							
	Buddha	Buddha2	Horses	Medieval	Mona	Papillon	StillLife	Average
Wanner and Goldluecke (2012a)	0.079	0.094	0.163	**0.111**	0.096	0.158	0.184	0.126
Tao *et al.* (2013)	0.103	0.102	**0.119**	0.133	0.127	0.273	0.198	0.151
Yu *et al.* (2013)	0.134	0.179	0.188	0.144	0.119	0.406	0.150	0.189
Chen *et al.* (2014)	**0.057**	0.139	0.122	0.129	**0.077**	**0.108**	**0.113**	**0.106**
Jeon *et al.* (2015)	0.094	**0.070**	0.129	0.123	0.081	0.237	0.135	0.124
Wang *et al.* (2015)	0.095	0.107	0.140	0.115	0.089	0.125	0.212	0.126

Bold numbers represent the best values in the corresponding column

The algorithms (Tao *et al.*, 2013; Yu *et al.*, 2013; Tosic and Berkner, 2014; Wanner and Goldluecke, 2014) that use all views can achieve good results on real light field data. However, the details of disparity are often smoothed. Chen *et al.* (2014) dynamically selected the unoccluded views during digital refocusing. Because the BCM of a fixed view varies from the refocus levels, the selected unoccluded views are also uncertain which decreases the robustness of the algorithm in noisy environments. The projection consistency found by Wang *et al.* (2015) is an important feature which guarantees that certain and enough unoccluded views are selected for depth estimation. This is why the BCM produces the best result on synthetic data but fails on real data. Because the light field has many more views than conventional multiview stereo, Williem and Park (2016) divided the angular patch into 3×3 subregions and proposed an angular entropy metric to select the subregion that is least polluted by noise and occluded views.

4.1.3 Glossy surface

Passive depth estimation for glossy objects such as metals, plastics, or ceramics has rarely been researched in light field. Because the classic photo-consistency assumption does not hold on glossy surface, the state-of-the-art algorithms perform poorly (Yu *et al.*, 2013; Chen *et al.*, 2014; Wanner and Goldluecke, 2014; Jeon *et al.*, 2015; Lin *et al.*, 2015; Wang *et al.*, 2015).

Johannsen *et al.* (2016) introduced sparse light field coding for specular surfaces. By learning the structure of the center view using dictionary learning and generating the light field atoms in the 4D space, the light field of a specular surface can be decomposed into different superimposed layers, which leverage depth estimation for these non-Lambertian areas. Tao *et al.* (2016) proposed a clustering method to eliminate specular pixels. Then the dichromatic model was adopted, and the consistency of the point and line was generalized from the photo-consistency measure to deal with the Lambertian surface and specular surface, respectively. However, artificial classification decreases the generality of the method for a glossy surface, and the dichromatic model fails to hold for metals. Wang *et al.* (2016a) analyzed diffuse plus single-lobe spatially varying (SV) bidirectional reflectance distribution functions (BRDFs) in the light field. By using the differential motion theory, they derived an SVBRDF-invariant equation relating depths and normals for a single-lobe BRDF that depends only on half-angles. By assuming a local polynomial prior on the surface, the shape and reflectance were both recovered. However, for general multilobe reflectance, this method has a few limitations.

In summary, depth estimation algorithms for the Lambertian surface have been well developed. Because the light field provides many more views than traditional multiview stereo matching, the key solution for the occlusion and noise problems is to select as many unoccluded views as possible. For a non-Lambertian surface, although some models or methods have been proposed, there is no theoretical solution until now, and it is still an open issue in light field depth estimation.

4.2 Super-resolution reconstruction

In the light field domain, spatial and angular resolutions are two aspects of a contradiction. A number of works on light field SR have been published in recent years. For didactic purpose, we classify the various techniques into two categories, namely, geometrically dependent and independent methods.

4.2.1 Geometrically dependent super-resolution reconstruction

Compared with the traditional 2D image-based SR, one of the advantages of light field is the capability of subpixel disparity estimation. The accuracy of the state-of-the-art depth estimation algorithms can reach 0.1 pixel (Table 1). Therefore, although the spatial resolution is decreased to trade the angular resolution in light field cameras, the images added from other views provide the possibility of recovering high-spatial-resolution images.

Bishop and Favaro (2012) analyzed the effect of aliasing in light field reconstruction and obtained both the depth and the high-resolution texture iteratively using a variational Bayesian framework. Wanner and Goldluecke (2012b) formulated view synthesis as a continuous inverse problem. The subpixel disparity map was estimated using structure tensor, and then the foreshortening effects caused by scene geometry transformations were correctly taken into account to improve both angular and spatial resolutions in the light field. Apart from these, Georgiev *et al.* (2011) and Yu *et al.* (2012) also made some useful explorations for geometrically dependent SR algorithms. All these methods need an input with 4D light field recordation. Recently, Zhang *et al.* (2015) proposed to reconstruct the 4D light field from a stereo pair. By introducing a disparity-assisted phase-based synthesis, they iteratively reconstructed the 4D light field. It opens a new idea for geometrically dependent SR.

4.2.2 Geometrically independent super-resolution reconstruction

The 4D light field is redundant, and there is a dimension gap between the 4D light field and the 3D world (Levin and Durand, 2010). This is the basis for geometrically independent SR. Levin and Durand (2010) found that the energy of the Fourier spectrum in a 4D light field focuses on a 3D subset and proposed to reconstruct the 4D light field by adding the Fourier spectrum of the 3D focal stack into the 4D light field. This idea was also adopted by Pérez *et al.* (2012). Another study shows the sparsity of the 4D light field (Shi *et al.*, 2014). By combining it with the idea of sparse Fourier transform, Shi *et al.* (2014) reconstructed the 4D light field from an angular-sparse light field.

Apart from the consideration of dimension gap, two hot tools, i.e., compressive sensing and deep learning, have been applied in light field SR. By placing a well-designed mask at the camera aperture, the rays from different angles were combined into the same image in a single shot, and the light field could be recovered via a Bayesian algorithm (Babacan *et al.*, 2012; Marwah *et al.*, 2013), Yoon *et al.* (2015) and Kalantari *et al.* (2016) trained a deep neural network using a large number of light fields for spatial and angular SR, respectively.

5 Light field applications

Unlike traditional imaging systems that lose the diversity between different rays, light field cameras capture rays from different angles. Apart from this, the BRDF can be estimated from multiview representations in the light field, which provides new approaches to analyze the elements in nature, such as liquids or cells. We review recent developments of light field in various disciplines, such as informatics, physics, medicine, and biology.

5.1 Informatics

A number of light field based applications have been developed in computer graphics, computer vision, and security areas. All these applications show great advantages compared with traditional methods.

In computer graphics, the light field is an important tool in rendering, stitching, and segmentation. Light field rendering is geometry independent, which does not require depth estimation (Shum and Kang, 2000; Buehler *et al.*, 2001). Classic digital refocusing (Ng, 2006) is capable of refocusing images in a fixed depth. Generalized volumetric focus (Dansereau *et al.*, 2015) can even refocus images in a depth range. Because the depth is embedded in the light field, panoramic light field theoretically removes the outliers due to parallax (Birklbauer *et al.*, 2013; Birklbauer and Bimber, 2014; Guo *et al.*, 2016) and improves the stitching results. On the basis of digital refocusing, the object can be segmented from a complex natural environment instead of from a background with pure colors (Maeno *et al.*, 2013; Edussooriya, 2015; Xu *et al.*, 2015; Mihara *et al.*, 2016), which improves the editing techniques in film making (Lytro Inc., 2011) (Fig. 7).

In computer vision, the light field has benefitted saliency detection, scene flow estimation, and material recognition. The introduction of focusness improves the accuracy of saliency detection in object boundaries to a great extent (Li *et al.*, 2014; Zhang *et al.*, 2015). In scene flow estimation, the light distribution in a higher 4D space provides a more accurate comparison between patches at different time and thereby provides a more precise scene flow estimation in environments of varying illuminations for motion analysis (Iffa *et al.*, 2012; Srinivasan *et al.*, 2015). Apart from these, the SVBRDF invariance of a glossy surface has been applied in material recognition (Wang *et al.*, 2016b), which achieves a 7% boost compared with the traditional 2D image-based method.

In the security area, one of the most important applications is 'seeing through occlusion' (Isaksen *et al.*, 2000) (Fig. 8). If the size of the synthetic aperture is larger than the occluder, the occluder will be blurred when the light field is refocused to the depth of the scene. Latter studies (Vaish *et al.*, 2006; Xiao *et al.*, 2014) have improved the basic method by selecting the unoccluded views for digital refocusing. Apart from this, the light field based flat surface detection has been well researched in face-based authentication systems (Ghasemi and Vetterli, 2014; Kim *et al.*, 2014; Raghavendra *et al.*, 2015).

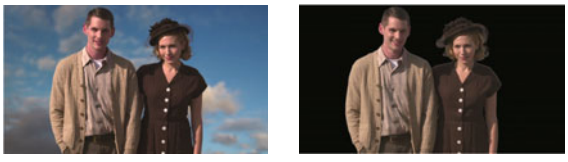

Fig. 7 Object segmentation in light fields (Lytro Inc., 2011): (a) original scene; (b) segmented human

Fig. 8 Seeing through occlusion (Vaish, 2007): (a) image from one view; (b) synthetic aperture image

5.2 Physics

PIV is an important issue in hydromechanics, and a number of methods have been developed, such as the defocusing digital PIV, tomographic PIV, and holographic PIV. However, there are two weaknesses in traditional methods, i.e., low seeding density and small volume size. Synthetic aperture PIV overcomes the inherent challenges of 3D PIV and shows the ability to reconstruct fields with high seeding density and large volume size (Belden *et al.*, 2010; Fahringer and Thurow, 2012; Thurow and Fahringer, 2013) (Fig. 9). By combining it with multiple light sheet illumination, two-component velocity measurements on multiple planes can also be achieved (Skupsch and Brücker, 2013).

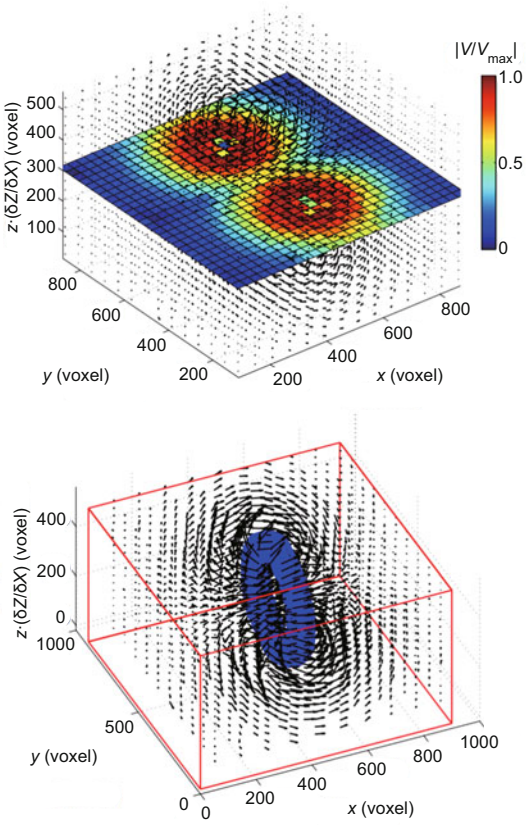

Fig. 9 Three-dimensional vector field resulting from particle image velocimetry (PIV) processing using synthetic aperture PIV (Belden *et al.*, 2010)

The measurement of a flame's 3D radiant energy field plays an important role in the analysis of the combustion process. Compared with the traditional computed tomography (CT), light field photography can theoretically achieve the synchronous acquisi-

tion of optical field information at large projection angles, which is more suitable for detecting the temperature of an exhaust plume. Yuan *et al.* (2016) analyzed the optical fields of participating media, such as absorbing, scattering, and emitting media. They summarized advantages and disadvantages of obtaining the emission characteristics and the temperature field using light field cameras. Based on this, Niu *et al.* (2016) further developed a generalized source multiflux method, which is faster and more accurate than those in previous studies, to simulate outgoing radiative intensities in arbitrary directions at the boundary surfaces of absorbing, emitting, and scattering media.

5.3 Medicine and biology

Because light field cameras can provide multiview images and the depth map in a single shot, it is suitable for observing moving or light-sensitive specimens using light field cameras. Levoy *et al.* (2006) built the first light field microscope by replacing the eyepiece in a traditional microscope with a microlens array and a camera sensor (Fig. 10). They obtained perspective views, focal stacks, and 3D reconstructions for a variety of biological specimens. Broxton *et al.* (2013) introduced the wave optics theory for the light field microscopy model, which leads to higher spatial resolution and better optical sectioning. Mignard-Debise and Ihrke (2015) explored an inexpensive light field microscope by replacing the previous microlens array and the camera sensor with a Lytro camera directly.

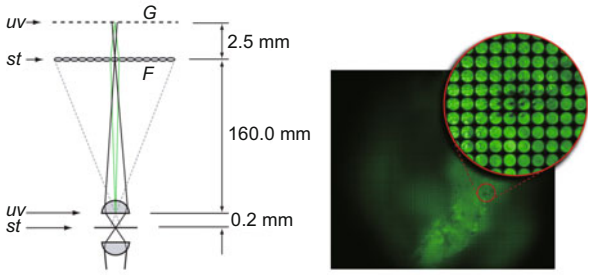

Fig. 10 Light field microscope and the captured light field of the specimen (Levoy *et al.*, 2006)

Apart from the MLA-based light field microscopy, Orth and Crozier (2013) introduced light field moment imaging (LFMI) in the design of the microscope. The scene was shot twice at different focus depths and the 4D light field was obtained by solving a Poisson equation. Liu *et al.* (2015) reduced the noise and errors in LFMI by increasing the number of shots.

6 Conclusions

Light field imaging theory is a hot spot in computational photography and brings revolutionary innovations to traditional digital imaging technologies. By using light field cameras, we have changed the ways of sensing, observing, and cognizing the physical world.

To further extend the applications of light field, it is necessary to calibrate light field cameras accurately and register multiview light fields to improve both the field of view and depth of field. The bottleneck of spatial and angular resolutions has been solved gradually by compressive sensing and using a high-dimensional deconvolution filter. Considering that there are various depth cues in a single shot of light field cameras, it is possible to fuse multiple depth cues to obtain high-accuracy 3D reconstruction and SR. The theoretical outcomes of light field processing will arouse significant revolutions for the core problems in computer vision and promote the applications of light field theory and imaging technology in some important domains, such as anti-terrorism surveillance, industrial inspection, novel medical imaging, augmented reality, and future media.

References

Babacan, S.D., Ansorge, R., Luessi, M., *et al.*, 2012. Compressive light field sensing. *IEEE Trans. Image Process.*, **21**(12):4746-4757. https://doi.org/10.1109/tip.2012.2210237

Belden, J., Truscott, T.T., Axiak, M.C., *et al.*, 2010. Three-dimensional synthetic aperture particle image velocimetry. *Meas. Sci. Technol.*, **21**(12):125403. https://doi.org/10.1088/0957-0233/21/12/125403

Bergamasco, F., Albarelli, A., Cosmo, L., *et al.*, 2015. Adopting an unconstrained ray model in light-field cameras for 3D shape reconstruction. Proc. IEEE Conf. on Computer Vision and Pattern Recognition, p.3003-3012. https://doi.org/10.1109/cvpr.2015.7298919

Birklbauer, C., Bimber, O., 2014. Panorama light-field imaging. *Comput. Graph. Forum*, **33**(2):43-52. https://doi.org/10.1111/cgf.12289

Birklbauer, C., Opelt, S., Bimber, O., 2013. Rendering gigaray light fields. *Comput. Graph. Forum*, **32**(2pt4):469-478. https://doi.org/10.1111/cgf.12067

Bishop, T.E., Favaro, P., 2012. The light field camera: extended depth of field, aliasing, and superresolution.

IEEE Trans. Patt. Anal. Mach. Intell., **34**(5):972-986. https://doi.org/10.1109/tpami.2011.168

Bok, Y., Jeon, H.G., Kweon, I.S., 2014. Geometric calibration of micro-lens-based light-field cameras using line features. Proc. European Conf. on Computer Vision, p.47-61. https://doi.org/10.1007/978-3-319-10599-4_4

Broxton, M., Grosenick, L., Yang, S., *et al.*, 2013. Wave optics theory and 3-D deconvolution for the light field microscope. *Opt. Expr.*, **21**(21):25418-25439. https://doi.org/10.1364/oe.21.025418

Buehler, C., Bosse, M., McMillan, L., *et al.*, 2001. Unstructured lumigraph rendering. Proc. 28th Annual Conf. on Computer Graphics and Interactive Techniques, p.425-432. https://doi.org/10.1145/383259.383309

Chen, C., Lin, H., Yu, Z., *et al.*, 2014. Light field stereo matching using bilateral statistics of surface cameras. Proc. IEEE Conf. on Computer Vision and Pattern Recognition, p.1518-1525. https://doi.org/10.1109/cvpr.2014.197

Cho, D., Lee, M., Kim, S., *et al.*, 2013. Modeling the calibration pipeline of the Lytro camera for high quality light-field image reconstruction. Proc. IEEE Int. Conf. on Computer Vision, p.3280-3287. https://doi.org/10.1109/iccv.2013.407

Dansereau, D.G., Pizarro, O., Williams, S.B., 2013. Decoding, calibration and rectification for lenselet-based plenoptic cameras. Proc. IEEE Conf. on Computer Vision and Pattern Recognition, p.1027-1034. https://doi.org/10.1109/cvpr.2013.137

Dansereau, D.G., Pizarro, O., Williams, S.B., 2015. Linear volumetric focus for light field cameras. *ACM Trans. Graph.*, **34**(2):15.1-15.20. https://doi.org/10.1145/2665074

Edussooriya, C.U.S., 2015. Low-Complexity Multidimensional Filters for Plenoptic Signal Processing. PhD Thesis, University of Victoria, Canada. http://hdl.handle.net/1828/6894

Fahringer, T., Thurow, B.S., 2012. Tomographic reconstruction of a 3-D flow field using a plenoptic camera. Proc. 42nd AIAA Fluid Dynamics Conf. and Exhibit, p.1-13. https://doi.org/10.2514/6.2012-2826

Georgiev, T., Lumsdaine, A., 2009. Superresolution with Plenoptic 2.0 cameras. Proc. Frontiers in Optics / Laser Science XXV / Fall OSA Optics & Photonics Technical Digest. https://doi.org/10.1364/srs.2009.stua6

Georgiev, T., Lumsdaine, A., 2010. Focused plenoptic camera and rendering. *J. Electron. Imag.*, **19**(2):021106. https://doi.org/10.1117/1.3442712

Georgiev, T., Lumsdaine, A., 2012. The multifocus plenoptic camera. Proc. Digital Photography VIII. https://doi.org/10.1117/12.908667

Georgiev, T., Zheng, K.C., Curless, B., *et al.*, 2006. Spatio-angular resolution tradeoffs in integral photography. Proc. 17th Eurographics Conf. on Rendering Techniques, p.263-272. https://doi.org/10.2312/EGWR/EGSR06/263-272

Georgiev, T., Chunev, G., Lumsdaine, A., 2011. Superresolution with the focused plenoptic camera. Proc. Computational Imaging IX, p.78730X. https://doi.org/10.1117/12.872666

Ghasemi, A., Vetterli, M., 2014. Detecting planar surface using a light-field camera with application to distinguishing real scenes from printed photos. Proc. IEEE Int. Conf. on Acoustics, Speech and Signal Processing, p.4588-4592. https://doi.org/10.1109/icassp.2014.6854471

Gortler, S.J., Grzeszczuk, R., Szeliski, R., *et al.*, 1996. The lumigraph. Proc. 23rd Annual Conf. on Computer Graphics and Interactive Techniques, p.43-54. https://doi.org/10.1145/237170.237200

Guo, X., Yu, Z., Kang, S.B., *et al.*, 2016. Enhancing light fields through ray-space stitching. *IEEE Trans. Vis. Comput. Graph.*, **22**(7):1852-1861. https://doi.org/10.1109/tvcg.2015.2476805

Hahne, C., Aggoun, A., Haxha, S., *et al.*, 2014. Light field geometry of a standard plenoptic camera. *Opt. Expr.*, **22**(22):26659-26673. https://doi.org/10.1364/oe.22.026659

Hahne, C., Aggoun, A., Velisavljevic, V., 2015. The refocusing distance of a standard plenoptic photograph. Proc. 3DTV-Conf.: the True Vision-Capture, Transmission and Display of 3D Video, p.1-4. https://doi.org/10.1109/3dtv.2015.7169363

Iffa, E., Wetzstein, G., Heidrich, W., 2012. Light field optical flow for refractive surface reconstruction. Proc. Applications of Digital Image Processing XXXV, p.84992H. https://doi.org/10.1117/12.981608

Isaksen, A., McMillan, L., Gortler, S.J., 2000. Dynamically reparameterized light fields. Proc. 27th Annual Conf. on Computer Graphics and Interactive Techniques, p.297-306. https://doi.org/10.1145/344779.344929

Jeon, H.G., Park, J., Choe, G., *et al.*, 2015. Accurate depth map estimation from a lenslet light field camera. Proc. IEEE Conf. on Computer Vision and Pattern Recognition, p.1547-1555. https://doi.org/10.1109/cvpr.2015.7298762

Johannsen, O., Heinze, C., Goldluecke, B., *et al.*, 2013. On the calibration of focused plenoptic cameras. *In*: Grzegorzek, M., Theobalt, C., Koch, R., *et al.* (Eds.), Time-of-Flight and Depth Imaging: Sensors, Algorithms, and Applications, p.302-317. https://doi.org/10.1007/978-3-642-44964-2_15

Johannsen, O., Sulc, A., Goldluecke, B., 2015. On linear structure from motion for light field cameras. Proc. IEEE Int. Conf. on Computer Vision, p.720-728. https://doi.org/10.1109/iccv.2015.89

Johannsen, O., Sulc, A., Goldluecke, B., 2016. What sparse light field coding reveals about scene structure. Proc. IEEE Conf. on Computer Vision and Pattern Recognition, p.3262-3270. https://doi.org/10.1109/cvpr.2016.355

Kalantari, N.K., Wang, T.C., Ramamoorthi, R., 2016. Learning-based view synthesis for light field cameras. *ACM Trans. Graph.*, **35**(6):193.1-193.10. https://doi.org/10.1145/2980179.2980251

Kim, C., Zimmer, H., Pritch, Y., *et al.*, 2013. Scene reconstruction from high spatio-angular resolution light fields. *ACM Trans. Graph.*, **32**(4):73.1-73.12. https://doi.org/10.1145/2461912.2461926

Kim, S., Ban, Y., Lee, S., 2014. Face liveness detection using a light field camera. *Sensors*, **14**(12):22471-22499. https://doi.org/10.3390/s141222471

Landy, M., Movshon, J.A., 1991. The Plenoptic Function and the Elements of Early Vision. MIT Press, USA, p.3-20.

Levin, A., Durand, F., 2010. Linear view synthesis using a dimensionality gap light field prior. Proc. IEEE Conf. on Computer Vision and Pattern Recognition, p.1831-1838. https://doi.org/10.1109/cvpr.2010.5539854

Levin, A., Fergus, R., Durand, F., *et al.*, 2007. Image and depth from a conventional camera with a coded aperture. *ACM Trans. Graph.*, **26**(3):70. https://doi.org/10.1145/1239451.1239521

Levoy, M., Hanrahan, P., 1996. Light field rendering. Proc. 23rd Annual Conf. on Computer Graphics and Interactive Techniques, p.31-42. https://doi.org/10.1145/237170.237199

Levoy, M., Ng, R., Adams, A., *et al.*, 2006. Light field microscopy. *ACM Trans. Graph.*, **25**(3):924-934. https://doi.org/10.1145/1141911.1141976

Li, J., Lu, M., Li, Z.N., 2015. Continuous depth map reconstruction from light fields. *IEEE Trans. Image Process.*, **24**(11):3257-3265. https://doi.org/10.1109/tip.2015.2440760

Li, N., Ye, J., Ji, Y., *et al.*, 2014. Saliency detection on light field. Proc. IEEE Conf. on Computer Vision and Pattern Recognition, p.2806-2813. https://doi.org/10.1109/cvpr.2014.359

Liang, C.K., Shih, Y.C., Chen, H.H., 2011. Light field analysis for modeling image formation. *IEEE Trans. Image Process.*, **20**(2):446-460. https://doi.org/10.1109/tip.2010.2063036

Lin, H., Chen, C., Kang, S.B., *et al.*, 2015. Depth recovery from light field using focal stack symmetry. Proc. IEEE Int. Conf. on Computer Vision, p.3451-3459. https://doi.org/10.1109/iccv.2015.394

Liu, J., Xu, T., Yue, W., *et al.*, 2015. Light-field moment microscopy with noise reduction. *Opt. Expr.*, **23**(22):29154-29162. https://doi.org/10.1364/OE.23.029154

Lumsdaine, A., Georgiev, T., 2008. Full Resolution Lightfield Rendering. Indiana University and Adobe Systems, Technical Report.

Lytro Inc., 2011. Lytro Cinema Brings Revolutionary Light Field Technology to Film and TV Production. Technical Report. http://www.lytro.com

Maeno, K., Nagahara, H., Shimada, A., *et al.*, 2013. Light field distortion feature for transparent object recognition. Proc. IEEE Conf. on Computer Vision and Pattern Recognition, p.2786-2793. https://doi.org/10.1109/cvpr.2013.359

Marwah, K., Wetzstein, G., Bando, Y., *et al.*, 2013. Compressive light field photography using overcomplete dictionaries and optimized projections. *ACM Trans. Graph.*, **32**(4):46.1-46.12. https://doi.org/10.1145/2461912.2461914

Maximilian, D., 2016. Light-Field Imaging and Heterogeneous Light Fields. PhD Thesis, Heidelberg University, Germany.

Mignard-Debise, L., Ihrke, I., 2015. Light-field microscopy with a consumer light-field camera. Proc. Int. Conf. on 3D Vision, p.335-343. https://doi.org/10.1109/3dv.2015.45

Mihara, H., Funatomi, T., Tanaka, K., *et al.*, 2016. 4D light field segmentation with spatial and angular consistencies. Proc. Int. Conf. on Computational Photography, p.54-61. https://doi.org/10.1109/iccphot.2016.7492872

Ng, R., 2005. Fourier slice photography. *ACM Trans. Graph.*, **24**(3):735-744. https://doi.org/10.1145/1073204.1073256

Ng, R., 2006. Digital Light Field Photography. PhD Thesis, Stanford University, USA.

Ng, R., Levoy, M., Brédif, M., *et al.*, 2005. Light Field Photography with a Hand-Held Plenoptic Camera. Technical Report, CTSR 2005-02, Stanford University, USA.

Niu, C.Y., Qi, H., Huang, X., *et al.*, 2016. Efficient and robust method for simultaneous reconstruction of the temperature distribution and radiative properties in absorbing, emitting, and scattering media. *J. Quant. Spectros. Rad. Transfer*, **184**:44-57. https://doi.org/10.1016/j.jqsrt.2016.06.032

Orth, A., Crozier, K.B., 2013. Light field moment imaging. *Opt. Lett.*, **38**(15):2666-2668. https://doi.org/10.1364/ol.38.002666

Perwaß, C., Wietzke, L., 2012. Single lens 3D-camera with extended depth-of-field. Proc. Human Vision and Electronic Imaging XVII. https://doi.org/10.1117/12.909882

Perwaß, U., Perwaß, C., 2013. Digital Imaging System, Plenoptic Optical Device and Image Data Processing Method. US Patents.

Pérez, F., Pérez, A., Rodríguez, M., *et al.*, 2012. Fourier slice super-resolution in plenoptic cameras. Proc. IEEE Int. Conf. on Computational Photography, p.1-11. https://doi.org/10.1109/iccphot.2012.6215210

Raghavendra, R., Raja, K.B., Busch, C., 2015. Presentation attack detection for face recognition using light field camera. *IEEE Trans. Image Process.*, **24**(3):1060-1075. https://doi.org/10.1109/tip.2015.2395951

Sabater, N., Drazic, V., Seifi, M., *et al.*, 2014. Light-Field Demultiplexing and Disparity Estimation. Technical Report, Technicolor Research and Innovation, France.

Seifi, M., Sabater, N., Drazic, V., *et al.*, 2014. Disparity-guided demosaicking of light field images. Proc. IEEE Int. Conf. on Image Processing, p.5482-5486. https://doi.org/10.1109/icip.2014.7026109

Shi, L., Hassanieh, H., Davis, A., *et al.*, 2014. Light field reconstruction using sparsity in the continuous Fourier domain. *ACM Trans. Graph.*, **34**(1):12.1-12.13. https://doi.org/10.1145/2682631

Shum, H., Kang, S.B., 2000. Review of image-based rendering techniques. Proc. Visual Communications and Image Processing, p.2-13. https://doi.org/10.1117/12.386541

Skupsch, C., Brücker, C., 2013. Multiple-plane particle image velocimetry using a light-field camera. *Opt. Expr.*, **21**(2):1726-1740. https://doi.org/10.1364/oe.21.001726

Srinivasan, P.P., Tao, M.W., Ng, R., *et al.*, 2015. Oriented light-field windows for scene flow. Proc. IEEE Int. Conf. on Computer Vision, p.3496-3504. https://doi.org/10.1109/iccv.2015.399

Tao, M.W., Hadap, S., Malik, J., *et al.*, 2013. Depth from combining defocus and correspondence using light-field cameras. Proc. IEEE Int. Conf. on Computer Vision, p.673-680. https://doi.org/10.1109/iccv.2013.89

Tao, M.W., Su, J.C., Wang, T.C., *et al.*, 2016. Depth estimation and specular removal for glossy surfaces using point and line consistency with light-field cameras. *IEEE Trans. Patt. Anal. Mach. Intell.*, **38**(6):1155-1169. https://doi.org/10.1109/tpami.2015.2477811

Thomason, C.M., Thurow, B.S., Fahringer, T., 2014. Calibration of a microlens array for a plenoptic camera. Proc. 52nd Aerospace Sciences Meeting, p.1456-1460. https://doi.org/10.2514/6.2014-0396

Thurow, B.S., Fahringer, T., 2013. Recent development of volumetric PIV with a plenoptic camera. Proc. 10th Int. Symp. on Particle Image Velocimetry, p.1-7.

Tosic, I., Berkner, K., 2014. Light field scale-depth space transform for dense depth estimation. Proc. IEEE Conf. on Computer Vision and Pattern Recognition, p.435-442. https://doi.org/10.1109/cvprw.2014.71

Vaish, V., 2007. Synthetic Aperture Imaging Using Dense Camera Arrays. PhD Thesis, Stanford University, USA.

Vaish, V., Garg, G., Talvala, E., *et al.*, 2005. Synthetic aperture focusing using a shear-warp factorization of the viewing transform. Proc. IEEE Computer Society Conf. on Computer Vision and Pattern Recognition, **3**:129. https://doi.org/10.1109/cvpr.2005.537

Vaish, V., Levoy, M., Szeliski, R., *et al.*, 2006. Reconstructing occluded surfaces using synthetic apertures: stereo, focus and robust measures. Proc. IEEE Computer Society Conf. on Computer Vision and Pattern Recognition, p.2331-2338. https://doi.org/10.1109/cvpr.2006.244

Venkataraman, K., Lelescu, D., Duparré, J., *et al.*, 2013. PiCam: an ultra-thin high performance monolithic camera array. *ACM Trans. Graph.*, **32**(6):166.1-166.13. https://doi.org/10.1145/2508363.2508390

Wang, T.C., Efros, A.A., Ramamoorthi, R., 2015. Occlusion-aware depth estimation using light-field cameras. Proc. IEEE Int. Conf. on Computer Vision, p.3487-3495. https://doi.org/10.1109/iccv.2015.398

Wang, T.C., Chandraker, M., Efros, A.A., *et al.*, 2016a. SVBRDF-invariant shape and reflectance estimation from light-field cameras. Proc. IEEE Conf. on Computer Vision and Pattern Recognition, p.5451-5459. https://doi.org/10.1109/cvpr.2016.588

Wang, T.C., Zhu, J.Y., Hiroaki, E., *et al.*, 2016b. A 4D light-field dataset and CNN architectures for material recognition. Proc. European Conf. on Computer Vision, p.121-138. https://doi.org/10.1007/978-3-319-46487-9_8

Wanner, S., Goldluecke, B., 2012a. Globally consistent depth labeling of 4D light fields. Proc. IEEE Conf. on Computer Vision and Pattern Recognition, p.41-48. https://doi.org/10.1109/cvpr.2012.6247656

Wanner, S., Goldluecke, B., 2012b. Spatial and angular variational super-resolution of 4D light fields. Proc. European Conf. on Computer Vision, p.608-621. https://doi.org/10.1007/978-3-642-33715-4_44

Wanner, S., Goldluecke, B., 2014. Variational light field analysis for disparity estimation and super-resolution. *IEEE Trans. Patt. Anal. Mach. Intell.*, **36**(3):606-619. https://doi.org/10.1109/tpami.2013.147

Wanner, S., Fehr, J., Jähne, B., 2011. Generating EPI representations of 4D light fields with a single lens focused plenoptic camera. Proc. Int. Symp. on Visual Computing, p.90-101. https://doi.org/10.1007/978-3-642-24028-7_9

Wanner, S., Meister, S., Goldluecke, B., 2013. Datasets and benchmarks for densely sampled 4D light fields. *In*: Bronstein, M., Favre, J., Hormann, K. (Eds.), Vision, Modeling and Visualization, p.225-226. https://doi.org/10.2312/PE.VMV.VMV13.225-226

Wilburn, B., 2004. High Performance Imaging Using Arrays of Inexpensive Cameras. PhD Thesis, Stanford University, USA.

Williem, W., Park, I.K., 2016. Robust light field depth estimation for noisy scene with occlusion. Proc. IEEE Conf. on Computer Vision and Pattern Recognition, p.4396-4404. https://doi.org/10.1109/cvpr.2016.476

Xiao, Z., Wang, Q., Si, L., *et al.*, 2014. Reconstructing scene depth and appearance behind foreground occlusion using camera array. Proc. IEEE Int. Conf. on Image Processing, p.41-45. https://doi.org/10.1109/icip.2014.7025007

Xu, Y., Nagahara, H., Shimada, A., *et al.*, 2015. TransCut: transparent object segmentation from a light-field image. Proc. IEEE Int. Conf. on Computer Vision, p.3442-3450. https://doi.org/10.1109/iccv.2015.393

Yoon, Y., Jeon, H.G., Yoo, D., *et al.*, 2015. Learning a deep convolutional network for light-field image super-resolution. Proc. IEEE Int. Conf. on Computer Vision, p.24-32. https://doi.org/10.1109/iccvw.2015.17

Yu, J., McMillan, L., 2004. General linear cameras. Proc. European Conf. on Computer Vision, p.14-27. https://doi.org/10.1007/978-3-540-24671-8_2

Yu, Z., Yu, J., Lumsdaine, A., *et al.*, 2012. An analysis of color demosaicing in plenoptic cameras. Proc. IEEE Conf. on Computer Vision and Pattern Recognition, p.901-908. https://doi.org/10.1109/cvpr.2012.6247764

Yu, Z., Guo, X., Lin, H., *et al.*, 2013. Line assisted light field triangulation and stereo matching. Proc. IEEE Int. Conf. on Computer Vision, p.2792-2799. https://doi.org/10.1109/iccv.2013.347

Yuan, Y., Liu, B., Li, S., *et al.*, 2016. Light-field-camera imaging simulation of participatory media using Monte Carlo method. *Int. J. Heat Mass Transfer*, **102**:518-527. https://doi.org/10.1016/j.ijheatmasstransfer.2016.06.053

Zhang, C., Ji, Z., Wang, Q., 2016. Rectifying projective distortion in 4D light field. Proc. IEEE Int. Conf. on Image Processing, p.1464-1468. https://doi.org/10.1109/icip.2016.7532601

Zhang, Z., Liu, Y., Dai, Q., 2015. Light field from micro-baseline image pair. Proc. IEEE Conf. on Computer Vision and Pattern Recognition, p.3800-3809. https://doi.org/10.1109/cvpr.2015.7299004

Zhou, C., Miau, D., Nayar, S.K., 2012. Focal Sweep Camera for Space-Time Refocusing. Technical Report CUCS-021-12, Department of Computure Science, Columbia University, USA.